Quercetinase QueD of *Streptomyces* sp. FLA, a Monocupin Dioxygenase with a Preference for Nickel and Cobalt†

Hedda Merkens,‡ Reinhard Kappl,§ Roman P. Jakob,|| Franz X. Schmid,|| and Susanne Fetzner*,‡

Institut für Molekulare Mikrobiologie und Biotechnologie, Westfälische Wilhelms-Universität Münster, 48149 Münster, Germany, Fachrichtung 2.5 Biophysik, Universität des Saarlandes, Klinikum Geb. 76, 66421 Homburg/Saar, Germany, and Laboratorium für Biochemie, Universität Bayreuth, 95440 Bayreuth, Germany

Received July 25, 2008; Revised Manuscript Received September 25, 2008

ABSTRACT: Quercetinase (QueD) of *Streptomyces* sp. FLA is an enzyme of the monocupin family and catalyzes the 2,4-dioxygenolytic cleavage of the flavonol quercetin. After expression of the *queD* gene in *Escherichia coli*, high specific QueD activity was found in crude cell extracts when the growth medium was supplemented with $NiCl_2$ or $CoCl_2$, but not when Mn^{2+}, Fe^{2+}, Cu^{2+}, or Zn^{2+} was added. The metal occupancy of Ni- and Co-QueD purified from these cells was ≤50%, presumably due to strong overproduction of QueD in *E. coli*. Circular dichroism spectroscopy indicated the same folded structure with a high content of β-sheet for the Ni and Co protein. The apparent kinetic constants for quercetin of Ni-QueD ($k_{cat} = 40.1\ s^{-1}$, and $K_m = 5.75\ \mu M$) and Co-QueD ($k_{cat} = 7.6\ s^{-1}$, and $K_m = 0.96\ \mu M$) indicate similar catalytic efficiencies; however, the ~5-fold lower apparent K_m value of Ni-QueD for dioxygen suggests that the nickel enzyme performs better under physiological conditions. The pH dependence of $k_{cat,app}$ indicates that an ionizable group with a pK_a near 6.8 has to be deprotonated for catalysis. Electron paramagnetic resonance spectra of resting Co-QueD are indicative of a high-spin ($S = {}^3/_2$) Co^{2+} species in a tetrahedral or trigonal-bipyramidal coordination geometry. Anoxic binding of quercetin to QueD drastically altered the hyperfine pattern at $g \approx 6$ without changing the valence state of the Co(II) center and elicited a hypsochromic shift of UV−vis absorption band I of quercetin. On the basis of spectroscopic data, and considering the organic chemistry of flavonols, a nonredox role of the metal center in catalysis is discussed.

Flavonols like quercetin (3,5,7,3′,4′-pentahydroxyflavone) are polyphenolic substances produced by a wide range of vascular plants (*1*). Quercetin, which exhibits antioxidant and antibacterial properties (*2, 3*), is present in many edible fruits and vegetables and thus is a major bioflavonoid in the human diet. Due to the release of quercetin and other flavonoids from decomposing plant material and from root and leaf exudates (*4*−*6*), soil microorganisms are also exposed to these compounds. It is therefore not surprising that anaerobic and aerobic bacteria as well as fungi have evolved the ability to detoxify and degrade flavonols (*7*−*10*).

In the aerobic microbial metabolism of quercetin, the initial oxidative attack is catalyzed by quercetinase (EC 1.13.11.24), which, in a 2,4-dioxygenolytic ring cleavage reaction, forms carbon monoxide and the depside 2-protocatechuoylphloroglucinolcarboxylic acid (*11*−*17*) (Figure 1). Quercetinases from *Aspergillus japonicus* and *Bacillus subtilis* are metal-dependent enzymes belonging to the cupin superfamily (*13, 18*). The cupin domain consists of a characteristic β-barrel fold which comprises two conserved amino acid motifs, $G(X)_5HXH(X)_{3,4}E(X)_6G$ and $G(X)_5PXG(X)_2H(X)_3N$, separated by an intermotif region that varies in length from 11 to >100 amino acid residues (*19*). The glutamate and the two histidine residues of motif 1 together with the conserved histidine of motif 2 can ligate different divalent metal ions. Fungal quercetinases contain a mononuclear Cu(II) center (*11, 12, 17, 20*), whereas the enzyme from *B. subtilis*, at least when produced in *Escherichia coli*, is able to incorporate different metal ions while retaining some quercetinase activity, being most active with Mn(II) (*21*).

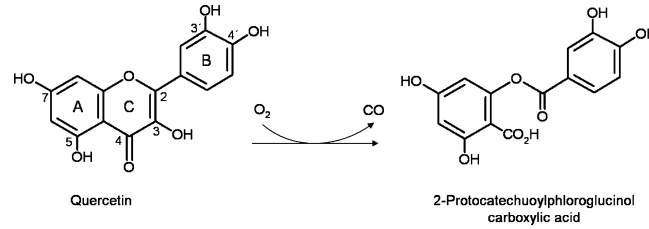

FIGURE 1: Reaction catalyzed by quercetinase (flavonol 2,4-dioxygenase).

† This work was supported by the Deutsche Forschungsgemeinschaft (FE 383/9). H.M. is also indebted to the University of Münster for a research grant.

* To whom correspondence should be addressed: Institut für Molekulare Mikrobiologie und Biotechnologie, Westfälische Wilhelms-Universität Münster, Corrensstrasse 3, D-48149 Münster, Germany. Telephone: +49-251-8339824. Fax: +49-251-8338388. E-mail: fetzner@uni-muenster.de.

‡ Westfälische Wilhelms-Universität Münster.

§ Universität des Saarlandes.

|| Universität Bayreuth.

10.1021/bi801398x CCC: $40.75
Published on Web 10/25/2008

Aci-reductone dioxygenase (ARD)[1] from *Klebsiella oxytoca* (formerly classified as *Klebsiella pneumoniae*) is another example for the promiscuity of the metal binding region of individual cupins. It is noteworthy that, depending on the cation in its active site, the ARD protein catalyzes two different reactions (*22*). Fe-ARD converts 1,2-dihydroxy-3-oxo-5-(methylthio)pent-1-ene, an intermediate of the methionine salvage pathway, to formate and 2-oxo-4-(methylthio)butyrate, the α-keto acid precursor of methionine. The same reaction is catalyzed by the Mg^{2+}-substituted enzyme. In contrast, Ni-ARD and the Co^{2+}- or Mn^{2+}-substituted forms in an off-pathway reaction catalyze the 1,3-dioxygenolytic cleavage of the same aci-reductone substrate to 3-(methylthio)propionate, carbon monoxide, and formate (*22*−*24*).

The quercetinases from *B. subtilis* and *A. japonicus* have a bicupin scaffold, each subunit consisting of 337 and 350 amino acids, respectively, which form two cupin domains (*13, 18*). In *Bacillus* quercetinase, each of these domains contains an active site metal ion (*14, 18*), whereas in the enzyme of *A. japonicus*, only the N-terminal domain of the bicupin subunit coordinates a Cu^{2+} ion (*13*). Recently, we identified the quercetinase gene *queD* of *Streptomyces* sp. strain FLA, which encodes a small protein of 186 amino acids that is 35.9 and 29.0% identical in sequence to the C-terminal and N-terminal cupin domains of *B. subtilis* quercetinase, respectively. The presence of two motifs matching the consensus sequences of the cupin superfamily as well as secondary structure predictions supported the hypothesis that QueD is a single-domain cupin (*16*).

To gain insight into the catalytic reaction and to contribute to a comparative analysis of different quercetinases, we set out to characterize the QueD protein of *Streptomyces* sp. FLA, especially with respect to its metal cofactor. In contrast to the enzymes from *B. subtilis*, *Aspergillus* spp., and *Penicillium olsonii*, this quercetinase is most active with Ni^{2+} ions as the cofactor, followed by Co^{2+}. QueD thus can be considered as the second Ni-dependent dioxygenase described so far, besides Ni-ARD. On the basis of spectroscopic data, a nonredox role of the metal center in catalysis is discussed for Ni- and Co-QueD.

EXPERIMENTAL PROCEDURES

Bacterial Strains, Plasmids, and Culture Conditions. E. coli BL21(DE3) (pLysS, pET23a-*queD*) (*16*) was grown at 37 °C in Luria-Bertani medium [LB (*25*)] containing ampicillin (100 μg/mL) and chloramphenicol (34 μg/mL), or in M9 minimal medium as specified below. *Streptomyces* sp. FLA (DSM 41951) (*16*) was grown at 30 °C in Standard I medium (Merck, Darmstadt, Germany).

Site-Directed Mutagenesis. Site-directed mutagenesis of the *queD* gene (GenBank accession number AM234612) was performed according to the protocol of the Phusion site-directed mutagenesis kit (Finnzymes, Espoo, Finland) using pET23a-*queD* as the template, Phusion Hot Start High-Fidelity DNA Polymerase (Finnzymes) for amplification, and the following primers: 5′-GACACCTACGCGGTCTTC-TAC-3′ and 5′-CGCGTGCGAGTGGGCGGG-3′ (the mismatch for generating the E76A replacement is underlined). Sequencing of both strands of the insert and flanking regions of the mutant plasmid was performed by MWG Biotech (Ebersberg, Germany).

Metal Dependence of QueD Activity in E. coli and Streptomyces sp. FLA. E. coli BL21(DE3) (pLysS, pET23a-*queD*) was grown in M9 minimal medium (*25*) at 37 °C to an optical density at 600 nm of 0.5. Subsequently, metal salts ($MnCl_2$, $FeCl_2$, $CoCl_2$, $NiCl_2$, $CuCl_2$, and $ZnCl_2$) were added to the cultures to a final concentration of 10 μM, and *queD* expression was induced with 1 mM isopropyl β-D-thiogalactopyranoside (IPTG). The cultivation temperature was reduced to 25 °C for 5 h and then shifted to 20 °C for an additional 15 h. Cells were harvested by centrifugation and stored at −80 °C. For the preparation of crude extracts containing the soluble proteins, cell pellets were resuspended in 50 mM Tris-HCl buffer (pH 7.5) containing 1 mM $MgCl_2$ and lysed with pLysS-encoded endogenous lysozyme. After DNA digestion for 1.5 h at 4 °C using 25 units of Benzonase (Novagen) per milliliter, the extract was centrifuged at 20000*g* for 30 min at 4 °C. Quercetinase activity was measured in the supernatant using the standard assay.

Streptomyces sp. FLA was grown at 30 °C for 1.5 days in Standard I medium. Cells were harvested by centrifugation, washed in sterile saline (0.5% NaCl and 0.012% $MgSO_4 \cdot 7H_2O$), resuspended in 200 mL of mineral salt medium (*26*) with a reduced NH_4Fe(III)citrate concentration of 1 μM, and supplemented with an SL6 trace element solution (100 μL/L) (*27*) and 1% glucose. After an additional 1.5 days of growth, cells were again harvested, washed, and used to inoculate 50 mL cultures of mineral salt medium (supplemented with an SL6 trace element solution and glucose) without NH_4Fe(III) citrate. These cultures were incubated for an additional day and subsequently supplied with 10 μM $MnCl_2$, $FeCl_2$, $CoCl_2$, $NiCl_2$, $CuCl_2$, or $ZnCl_2$ and with 2 mM quercetin to induce QueD synthesis. After induction for 24 h, cells were harvested and stored at −20 °C. For the preparation of crude extracts, cells resuspended in 50 mM Tris-HCl (pH 7) were disrupted by sonication. The extract was centrifuged at 20000*g* for 30 min at 4 °C, and supernatants were assayed for quercetinase activity.

Purification of Recombinant Hexahistidine-Tagged Ni- and Co-QueD. E. coli BL21(DE3) (pLysS, pET23a-*queD*) was grown in M9 medium as described above. For production of Ni- or Co-QueD, $NiCl_2$ or $CoCl_2$ was added to a final concentration of 10 μM, respectively, at the time of IPTG induction. For analysis of the composition of QueD synthesized in the presence of an excess supply of both metal ions, 10 μM $NiCl_2$ and 10 μM $CoCl_2$ were added simultaneously with IPTG. Preparation of crude cell extracts containing soluble proteins and purification of recombinant His_6-tagged proteins by metal chelate affinity chromatography were performed as described previously for recombinant $QueDHis_6$ from LB-grown cultures (*16*). Fractions exhibiting quercetinase activity were pooled, washed with 50 mM Tris-HCl (pH 8), concentrated by ultrafiltration, frozen in liquid nitrogen, and stored at −80 °C.

[1] Abbreviations: ARD, aci-reductone dioxygenase; CD, circular dichroism; EDTA, ethylenediaminetetraacetate; EPR, electron paramagnetic resonance; IPTG, isopropyl β-D-thiogalactopyranoside; LB, Luria-Bertani (lysogeny broth); PAGE, polyacrylamide gel electrophoresis; PCR, polymerase chain reaction; QueD, quercetinase (quercetin 2,4-dioxygenase); SDS, sodium dodecyl sulfate; Tris, tris(hydroxymethyl)aminomethane.

Protein Analysis. Protein concentrations were estimated using the Bradford method as modified by Zor and Selinger (*28*). Concentrations of electrophoretically pure QueD protein were deduced from the theoretical molar extinction coefficient ($\varepsilon_{280} = 15993\ M^{-1}\ cm^{-1}$) calculated using the method of Pace et al. (*29*). Denaturing (sodium dodecyl sulfate) polyacrylamide gel electrophoresis (SDS−PAGE) was performed as described by Laemmli (*30*), using an overall acrylamide concentration of 12.5% and a cross-linker concentration of 2.6% in the separating gels. Gel filtration of QueD proteins was performed on a Superdex 75 column (GE Healthcare, Freiburg, Germany) in 50 mM Tris-HCl buffer (pH 8) containing 150 mM NaCl; the gel filtration LMW calibration kit (GE Healthcare) was used as molecular mass standard. Covalent cross-linking of QueD with bis(sulfosuccinimidyl)suberate (BS^3; Pierce, Rockford, IL) was performed in 20 mM HEPES-NaOH (pH 8) according to the manufacturer's instructions. Molar ratios of protein to BS^3 were varied from 1:2.5 to 1:10.

Metal Analysis. Metal contents of purified QueD proteins were determined by inductively coupled plasma optical emission spectroscopy (ICP-OES) on a Thermo Jarrell-Ash Enviro 36 ICAP instrument by the Chemical Analysis Laboratory, Center for Applied Isotope Studies, University of Georgia (Athens, GA).

Enzyme Assays and Determination of Kinetic Parameters. QueD activity was determined spectrophotometrically by measuring quercetin consumption. The standard assay in a total volume of 1 mL contained 50 μL of 1.2 mM quercetin dissolved in dimethyl sulfoxide (DMSO) and appropriate amounts of protein in 50 mM Tris-HCl buffer (pH 8.0). One unit was defined as the amount of enzyme that converts 1 μmol of quercetin per minute at 22 °C ($\varepsilon_{367,pH\ 8} = 14850\ M^{-1}\ cm^{-1}$).

Assays for the determination of apparent steady-state kinetic parameters for quercetin were performed in air-saturated buffer [50 mM Tris-HCl (pH 8.0)] at 22 °C. The substrate concentrations were varied between 1.75 and 60 μM for Co-QueD and between 1.75 and 100 μM for Ni-QueD. Three independent series of measurements were performed for each protein, and each assay within a series was conducted in at least triplicate. For the determination of kinetic constants for dioxygen, reaction buffer [50 mM Tris-HCl (pH 8.0)] was brought to a temperature of 22 °C, saturated with O_2, air, or N_2, to obtain stock solutions with defined O_2 concentrations (1.27, 0.267, or 0 mM, respectively), and kept under the same atmosphere. The concentration of O_2 in dioxygen-saturated buffer was calculated on the basis of the solubility of oxygen in air-saturated water at 22 °C. Quercetin (1 mM in DMSO) and enzyme solutions were saturated with and kept under argon during the assays. A cuvette with a septum was flushed with argon prior to each measurement. Different O_2 concentrations (0.05−1.17 mM) were adjusted by mixing buffer stock solutions in the anoxic cuvette using gastight syringes, and substrate and enzyme solutions were added with syringes to start the reaction. For each QueD form, data from eight separate experiments were used to deduce the apparent kinetic constants for dioxygen. Apparent K_m and k_{cat} values of Ni- and Co-QueD for quercetin and of Ni-QueD for dioxygen were deduced from Hanes plots; the values for Co-QueD for O_2 were calculated using the Hill equation (*31*). For both Ni-QueD and Co-QueD, a single protein preparation was used for determination of apparent kinetic parameters, metal analysis, and EPR spectroscopy.

The pH dependence of Ni-QueD was determined in 50 mM MES-Tris buffer between pH 6 and 9 ($\varepsilon_{367,pH\ 6} = 19580\ M^{-1}\ cm^{-1}$; $\varepsilon_{367,pH\ 7} = 18650\ M^{-1}\ cm^{-1}$; $\varepsilon_{367,pH\ 8} = 14660\ M^{-1}\ cm^{-1}$; $\varepsilon_{367,pH\ 9} = 12380\ M^{-1}\ cm^{-1}$). For each pH value, three independent series of measurements were performed, and each assay within a series was conducted in triplicate. Using Origin (OriginLab Corp., Northhampton, MA), the profile of $\log(k_{cat})$ as a function of pH was fitted with the following equation, which describes a curve with one rate-increasing pK_a value:

$$\log(k_{cat}) = \log(k_{cat,max}) - \log(1 + 10^{pK_a - pH}) \quad (1)$$

The profile of $\log(k_{cat}/K_m)$ was fitted with eq 2, which describes a bell-shaped curve with one increasing and one decreasing pK_a value:

$$\log(k_{cat}/K_m) = \log(k_{cat}/K_m)_{max} - \log(1 + 10^{pK_a1 - pH} + 10^{pH - pK_a2}) \quad (2)$$

The activity of Ni- and Co-QueD toward different flavonols was determined by measuring oxygen consumption with a Clark-type oxygen electrode (Digital Model 10, Rank Brothers Ltd., Cambridge, England) as described previously (*16*). These assays were performed at pH 7 because myricetin rapidly decomposes at pH 8.

Identification of Products Formed from Quercetin. For detection of quercetinase-catalyzed carbon monoxide formation, the standard assay was carried out in a 1.5 mL reaction tube, with a filter paper soaked with a $PdCl_2$ solution (1:500, w/v) placed in the lid. The CO released in the enzyme-catalyzed reaction reduces Pd^{2+} to elemental palladium, which precipitates as a black solid.

To identify the organic product of the QueD-catalyzed reaction, 500 μg of quercetin was completely converted by the enzyme; the reaction was performed at pH 7 to prevent possible alkali-catalyzed hydrolysis. The organic product of the reaction was purified by combined anion exchange reversed-phase chromatography using the OASIS MAX sorbent (Waters, Milford, MA), according to the protocol of the manufacturer; the product was eluted from the column with 2% formic acid in methanol. The preparation was diluted in methanol and ammonium acetate and subjected to electrospray mass spectrometry, performed on a QUATTRO LCZ instrument (Waters-Micromass, Manchester, U.K.) at the Institute of Organic Chemistry, University of Münster.

To assess whether cleavage of quercetin possibly involves a 2,3-dioxygenolytic reaction resulting in formation of an α-keto acid, or side reactions to other keto compounds, the product of the enzyme-catalyzed conversion (performed at pH 7 and 8) was directly reacted with 2,4-dinitrophenylhydrazine (*32*). For the reaction at pH 7, for example, 6 μmol of quercetin was incubated for 1.5 h with 0.7 nmol of Ni-QueD or 3.5 nmol of Co-QueD in 5 mL of assay buffer. Subsequently, 2,4-dinitrophenylhydrazine (dissolved in 2 M HCl) was added to a final concentration of 0.017% (w/v), and the samples were incubated for 5 min. Alkaline conditions were adjusted by addition of NaOH, and 2,4-dinitrophenylhydrazones were detected spectrophotometrically at 440 nm. In a control reaction, the same amount of quercetin

was incubated in buffer in the absence of QueD and treated the same way. Each assay was performed in triplicate, and pyruvate was used as a reference α-keto acid for calibration. The detection limit was ~5 μM pyruvate.

UV−Vis Spectroscopy. UV−vis spectra for solutions of quercetin (30 μM), quercetin (30 μM) plus $NiCl_2$ or $CoCl_2$ (45 μM), and of anoxic mixtures of QueD proteins and quercetin were recorded in 50 mM MES-Tris buffer on a JASCO model V-550 spectrophotometer. For the estimation of molar concentrations of holoenzymes, we assumed that the total of Ni (0.55 atom per subunit) and Co (0.33 atom per subunit) is located in the active site of Ni- and Co-QueD, respectively. To adjust a 1.5-fold molar excess of holoenzyme over quercetin, the solution contained 82 μM Ni-QueD or 137 μM Co-QueD and 30 μM quercetin. Prior to being mixed in an anaerobic cuvette using gastight syringes, all solutions were repeatedly flushed with and kept under argon.

Circular Dichroism (CD) Spectroscopy. CD was measured with a JASCO J600A CD spectrometer equipped with a PTC 348 Peltier element. The CD spectra in the far-UV region were measured at a protein concentration of 5 μM in 10 mM potassium phosphate (pH 7.0) in 1 mm cells at a scan rate of 20 nm/min and a bandwidth of 1 nm. Spectra were measured 10 times and averaged. A secondary structure analysis was performed with K2D (*33*).

Electron Paramagnetic Resonance (EPR) Spectroscopy. Samples (150 μL) of Ni- or Co-QueD in 50 mM Tris-HCl (pH 8.0) were flushed with argon in an anaerobic glovebox, transferred in EPR quartz tubes (Wilmad), and directly frozen in liquid nitrogen. The concentration in the samples of 0.53 mM Ni-QueD and 1.13 mM Co-QueD corresponded to 0.3 mM Ni holoenzyme and 0.37 mM Co holoenzyme, based on Ni and Co contents of 0.55 and 0.33 atom per subunit, respectively, provided that the total of Ni and Co is in the active site. EPR spectra were recorded at X-band frequency (9.5 GHz) on a Bruker ESP300e spectrometer equipped with an Oxford ESR 900 helium flow cryostat and an ITC 4 temperature controller (Oxford Instruments). After (oxic as well as anoxic) measurement of the protein samples "as isolated", quercetin was added under anoxic conditions in an equimolar ratio, and in a 3-fold molar excess to the holoenzyme, and EPR spectra were recorded again. A third and fourth series of measurements were performed after the samples were exposed to air for 10 s and 5 min, respectively, in the EPR tube to allow QueD-catalyzed conversion of quercetin. The spectra were recorded for identical spectrometer settings: modulation amplitude of 0.7 mT, modulation frequency of 100 kHz, and microwave powers of 20 and 6.3 mW. The microwave frequency was measured with an HP 5350B frequency counter. The temperature was varied between 5 and 35 K; the presented spectra were obtained at 8 and 15 K, respectively. Spectra were accumulated for up to 3800 s, and a baseline was recorded for each experiment. The latter was used to remove the background signals of the setup. Spectra are presented in normalized mode, i.e., for the same receiver gain and number of accumulations. Integration was performed with Bruker WinEpr and XEPRView.

RESULTS

Quercetinase Activity in Cell Extract Supernatants of E. coli BL21(DE3) (pLysS, pET23a-queD) and Streptomyces sp. FLA as a Function of Metal Salts in the Growth Medium. For the heterologous synthesis of recombinant cupin proteins in *E. coli*, it has been described before that incorporation of the metal cofactor into the protein is drastically influenced by the divalent metal ions present in the culture medium (*21, 22*). As the specific activity of QueD purified from LB-grown recombinant *E. coli* was ~25-fold lower compared to that of "wild-type" QueD prepared from *Streptomyces* sp. FLA (*16*), we assumed that the composition of the LB medium, and the intracellular metal quotas of *E. coli* under these growth conditions, are not optimal for synthesis of catalytically competent QueD. Therefore, the *E. coli* expression clone was cultivated in minimal medium, and different metal dichlorides were added to the cultures upon induction of *queD* expression. The presence of Ni^{2+} and Co^{2+} in fact resulted in 16- and 7.6-fold increases, respectively, in QueD specific activity in cell extract supernatants ("crude extracts"), compared to a control culture without added metal ions in the medium. This increase in activity was specific for Ni^{2+} and Co^{2+}; it was not observed when Mn^{2+}, Fe^{2+}, Cu^{2+}, or Zn^{2+} was added to the culture medium. When an analogous experiment was performed with *Streptomyces* sp. FLA, specific quercetinase activities in crude extracts of cells grown in the presence of Mn^{2+}, Fe^{2+}, Cu^{2+}, or Zn^{2+} largely corresponded to those from cells grown without addition of metal ions. Supplementing the cultures of strain FLA with $NiCl_2$ and $CoCl_2$ resulted in 6.1- and 1.6-fold higher quercetinase activities in crude extracts, respectively. Taken together, the data suggest strongly that the QueD protein is most active with nickel as the cofactor.

Subunit Composition, Metal Contents, and CD Spectra of Recombinant QueD Proteins. The molecular mass of the hexahistidine-tagged QueD monomer, calculated from the amino acid sequence, is 23041 Da. On the basis of gel permeation chromatography, the molecular masses of native Ni- and Co-QueD were estimated to be 65.0 ± 0.4 and 65.1 ± 0.8 kDa, respectively, suggesting a homotrimeric subunit composition. After covalent cross-linking and analysis by SDS−PAGE, both proteins exhibited a prominent band with a molecular mass of 45 kDa, and weak bands of 66 kDa and of higher molecular masses; such weak bands could have resulted from intermolecular cross-linking. Thus, a dimeric structure of native QueD proteins also seems possible, as an elongated dimer might migrate with an apparent mass similar to that of a spherical trimer in gel filtration. The crystal structures of quercetinases of *B. subtilis* and *A. japonicus* indicate a homodimeric structure of these proteins (*13, 18*); however, their subunits are two-domain cupins, whereas the monomer of *Streptomyces* QueD was proposed to have a monocupin fold (*16*).

The recombinant hexahistidine-tagged QueD, purified from the *E. coli* expression clone grown in LB medium (*16*), contained 0.44 equiv of iron per monomer (Table 1). Iron and zinc are in fact the most abundant intracellular transition metal ions in *E. coli*, and cells of *E. coli* BW25113 cultivated in LB actually contained >0.1 mM iron (*34*). Metal ion concentrations in LB medium are >1 μM for Fe and Zn and <0.1 μM for Mn, Co, Ni, and Cu (*34*).

ICP-OES metal analyses of two independent preparations of QueD from cells grown in the presence of $NiCl_2$ yielded metal contents of ~0.5 equiv of Ni per subunit; the occupancy of Co-QueD preparations was similar (Table 1). Interestingly, metal analysis of "Ni-Co-QueD" (Table 1)

Table 1: Metal Contents of Individual Preparations of Recombinant *Streptomyces* QueD As Determined by ICP-OES

	no. of metal atoms per subunit				
metal	Fe-QueD[a]	Co-QueD[b] (two batches)	Ni-QueD[c] (two batches)	Ni-Co-QueD[d]	QueD-E76A[c]
Mn	0.023	0.002/0.001	0.003/0.002	0.001	0.002
Fe	0.435	0.038/nd[e]	0.135/0.038	0.022	0.021
Co	nd[e]	0.476/0.326	0.005/0.001	0.293	0.022
Ni	0.020	0.034/0.017	0.474/0.552	0.063	0.048
Cu	0.005	0.026/0.008	0.048/0.024	0.017	0.037
Zn	0.087	0.025/0.006	0.055/0.049	0.009	0.014

[a] Purified from *E. coli* BL21(DE3) (pLysS, pET23a-*queD*) grown in LB. [b] Purified from *E. coli* BL21(DE3) (pLysS, pET23a-*queD*) grown in minimal medium with 10 μM $CoCl_2$. [c] Purified from *E. coli* BL21(DE3) (pLysS, pET23a-*queD*) grown in minimal medium with 10 μM $NiCl_2$. [d] Purified from *E. coli* BL21(DE3) (pLysS, pET23a-*queD*) grown in minimal medium with $NiCl_2$ and $CoCl_2$ (10 μM each); metal salts were added to the medium upon induction of *queD* expression. [e] Not detected.

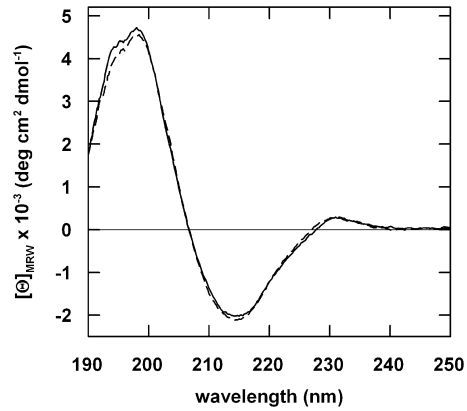

FIGURE 2: Far-UV CD spectra of (—) Co-QueD and (---) Ni-QueD at 25 °C. The spectra were recorded with 5 μM protein in 10 mM potassium phosphate (pH 7.0) with a path length of 1 mm and a bandwidth of 1 nm.

suggested that in the recombinant *E. coli* strain, Co^{2+} is incorporated preferentially into the cupin.

Ni-QueD and Co-QueD are well-folded proteins and have identical secondary structures. This is indicated by their CD spectra (Figure 2), which are virtually superimposable. The spectra exhibit minima near 217 nm and maxima near 198 nm. This is typical for proteins with a high content of β-sheet structure and a very low content of helices (*35*). The spectra in Figure 2 were analyzed with K2D (*33*). It indicates that both proteins consist of 5% α-helix and 48% β-sheet. These values are in good agreement with the values of 5% α-helix and 43% β-sheet, as calculated from the crystal structure of quercetinase of *B. subtilis* (*18*). This suggests that QueD from *Streptomyces* sp. FLA is similar in its structure to the homologous C-terminal and N-terminal cupin domains of the enzyme from *B. subtilis*, with which it is 35.9 and 29.0% identical in sequence, respectively.

Products of Quercetin Conversion Catalyzed by Ni-QueD and Co-QueD. Reduction of $PdCl_2$ by a gaseous product formed from quercetin by Ni- and Co-QueD suggested that both enzymes catalyze a 2,4-dioxygenolytic cleavage of the heterocyclic ring with release of carbon monoxide, as shown in Figure 1. The organic product from the enzymatic turnover of quercetin by both Ni- and Co-QueD was extracted by combined anion exchange reversed-phase chromatography and analyzed by electrospray mass spectrometry, indicating a compound with an ion at *m/z* 324.1 for $[M + NH_4]^+$. This is consistent with the chemical composition ($[C_{14}H_{10}O_8 + NH_4]^+$) of the ammonium adduct of protocatechuoylphloroglucinolcarboxylic acid, confirming that both QueD forms catalyze 2,4-dioxygenolysis of the heterocyclic ring. There was no evidence of the α-keto acid ($C_{15}H_{10}O_9$), which would result from 2,3-dioxygenolytic cleavage, being present in the extract. To examine the possibility that a keto compound might have been formed as side product, but lost during extraction, the aqueous enzyme assays after complete conversion of the substrate were directly reacted with 2,4-dinitrophenylhydrazine. On the basis of calibration of the assay with pyruvic acid hydrazone, the product from the conversion of 6 μmol of quercetin, catalyzed by Ni- and Co-QueD at pH 7, contained 0.039 ± 0.003 and 0.075 ± 0.011 μmol of a keto compound, respectively, corresponding to ~0.7 and ~1.3% of the side product, respectively. When the Ni- and Co-QueD-catalyzed reaction was performed at pH 8, ~1.3% of the side product was detected in both assays. However, besides the α-keto acid resulting from 2,3-dioxygenolytic cleavage, products such as 2,5,7,3′,4′-pentahydroxyflavan-3,4-dione, 2-(3,4-dihydroxybenzoyl)-2,4,6-trihydroxybenzofuran-3(2*H*)-one, and hydroxylated phenylglyoxylic acid, which have been observed to be formed in nonenzymatic, metal- or base-catalyzed oxidation of quercetin (*36, 37*), might also react to hydrazones. The side product was not detected in control experiments, but we cannot exclude the possibility that it is formed unspecifically, e.g., in an oxidation reaction mediated by transition metal ions adsorbed to the protein.

Activity and Steady-State Kinetic Parameters of QueD Proteins. The activity of the purified QueD proteins depends strongly on the nature of the metal ion cofactor. The specific activities of Co-QueD and Ni-QueD were 28 and 144 units/mg, respectively, whereas Fe-QueD, as purified from cells grown in LB medium, exhibited a specific activity of only 4 units/mg. Addition of different metal dichlorides to 100- and 1000-fold molar excesses over recombinant quercetinase did not increase enzymatic activity. Incubation of QueD at elevated temperatures (50−60 °C) with chelating agents (EDTA and *o*-phenanthroline), or with metal salt, also did not significantly change the activity of QueD, compared to protein samples incubated in the absence of effectors (data not shown). Since these experiments suggested that in vitro depletion and reconstitution of the metal cofactor of QueD are difficult, if not impossible, kinetic and spectroscopic data were collected for the QueD proteins as isolated from recombinant *E. coli*.

Even though the occupancy of metal ions is different in the three QueD forms (Table 1), the apparent kinetic parameters of Fe-QueD clearly show that iron is a poor cofactor (Table 2). Ni- and Co-QueD exhibit similar catalytic efficiencies (k_{cat}/K_m) for quercetin when enzyme activity is

Table 2: Apparent Kinetic Parameters for the Fe, Co, and Ni Forms of Recombinant QueD [in 50 mM Tris-HCl buffer (pH 8)] and Metal Occupancies (atom per QueD subunit) of the Protein Preparations[a]

metal	no. of atoms per subunit	$K_{m,app}$(quercetin) (μM)	$k_{cat,app}$(quercetin) (s^{-1})	$k_{cat,app}/K_{m,app}$(quercetin) (s^{-1} μM^{-1})	$K_{0.5,app}(O_2)$ (μM)	$k_{cat,app}(O_2)$ (s^{-1})	$k_{cat,app}/K_{0.5,app}(O_2)$ (s^{-1} μM^{-1})
Fe	0.44	14.1 ± 0.7[b]	1.5 ± 0.1[b]	0.1[b]	nd[c]	nd[c]	–
Co	0.33	0.96 ± 0.05	7.6 ± 0.5	7.9	1230±310[d]	12.5 ± 4.9	0.01
Ni	0.55	5.75 ± 0.12	40.1 ± 3.4	7.0	256 ± 45[e]	19.0 ± 3.5	0.07

[a] The same QueD preparations were used for EPR spectroscopy. [b] Data from ref *16*. [c] Not determined. [d] Hill equation. [e] Michaelis−Menten equation.

Table 3: Relative Activities of QueD Proteins toward Flavonols (3-hydroxyflavones)[a]

substrate	synonym	relative activity (%)		
		Fe-QueD[b]	Co-QueD	Ni-QueD
quercetin	3,5,7,3′,4′-pentahydroxyflavone	100	100	100
kaempferol	3,5,7,4′-tetrahydroxyflavone	70	43	29
myricetin	3,5,7,3′,4′,5′-hexahydroxyflavone	49	77	46
galangin	3,5,7-trihydroxyflavone	28	13	16
fisetin	3,7,3′,4′-tetrahydroxyflavone	23	35	15
morin	3,5,7,2′,4′-pentahydroxyflavone	1.7	5.5	0.9

[a] The activities of Fe-, Co-, and Ni-QueD for quercetin, defined as 100%, were 4, 28, and 144 units/mg, respectively. [b] Data from ref *16*.

measured in air-saturated buffer. The Co form has a low apparent K_m value but also a relatively low turnover number, whereas the high apparent k_{cat} of Ni-QueD is counteracted by a $K_{m,app}$ value that is 6-fold higher than that of Co-QueD (Table 2).

The saturation curve of Co-QueD for dioxygen did not follow Michaelis−Menten kinetics but was slightly sigmoidal. The formally calculated Hill coefficient with its standard deviation is 1.14 ± 0.07; however, this value is not sufficiently significant to support strict cooperativity. The $K_{m,app}$ of the Ni enzyme for dioxygen is ~5-fold lower than the $K_{0.5}$ value (the substrate concentration at half-saturation in the Hill equation) of Co-QueD (Table 2). Actually, the value for Ni-QueD of 256 μM is similar to the concentration of dioxygen dissolved in air-saturated water at ambient temperature, whereas $K_{0.5,app}$ for dioxygen of Co-QueD is close to the molar solubility of O_2 in water at 1 atm (~1.3 mM). Such a high $K_{0.5,app}$ should significantly restrain the catalytic performance of Co-QueD in vivo, i.e., at physiological O_2 concentrations. The apparent k_{cat} values for dioxygen are similar for both enzyme forms.

Both Ni- and Co-QueD are most active at 40 °C and exhibit an optimum of activity at pH 8. If the activities at pH 8 are set to 100%, the relative activities of Ni-QueD and Co-QueD at pH 6, 7, and 9 are 10 and 30%, 68 and 69%, and 47 and 46%, respectively. In contrast, Cu-quercetinases from *Aspergillus* spp. are most active at pH ~6 (*12, 20*). Both metal forms of *Streptomyces* QueD catalyze the cleavage of flavonols (Table 3), whereas the 2,3-dihydroflavonol taxifolin and the flavone luteolin are not converted, confirming that the C2−C3 double bond and the 3-OH group of the substrate are essential for catalysis. Among the substrates tested, quercetin is preferred by all three metal forms of QueD; however, the type of metal ion and/or subtle conformational differences in the protein forms appear to affect the relative activities toward flavonols that differ in their hydroxylation pattern at the A- and B-rings (Table 3).

pH Dependence of Ni-QueD. The pH dependence of the QueD-catalyzed reaction could be measured only between pH 6.5 and 9, because the activity of QueD is very low at pH <6.5, and because quercetin decomposes at pH >9. The log(k_{cat}) profile, which reflects ionizations of the enzyme−substrate (ES) complex, develops a plateau at pH >7 and decreases toward low pH values (Figure 3). Under the assumption that a single ionizable group is responsible for this pH dependence, the data were fitted with eq 1, indicating a maximum $k_{cat,app}$ of 47.4 ± 0.5 s^{-1} and a pK_a value for the ionizable group of 6.78 ± 0.03. This pK_a of ~6.8 could represent either an amino acid residue of the enzyme which participates in catalysis as an active site base or one of the hydroxyl groups of quercetin which must be unprotonated for catalysis. On the basis of spectrophotometric measurements, pK_a values for quercetin of 11.0, 9.9, 8.0, 7.1, and 5.7 were reported (*38*).

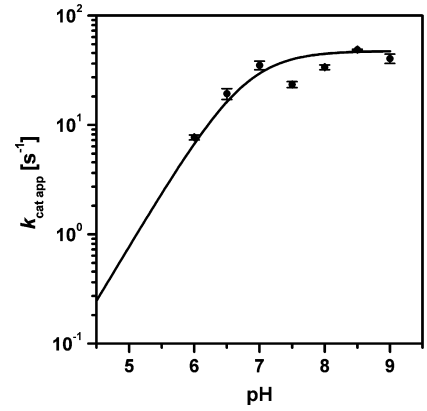

FIGURE 3: Variation of the apparent k_{cat}(quercetin) of Ni-QueD with pH. The solid line was plotted using eq 1.

Apparent K_m values of QueD were small at low pH (~2 μM at pH 6) and high at alkaline pH (~76 μM at pH 9). Because accurate determinations of K_m values at low and high pH would have required measurements at substrate concentrations well below and above the photometrically measurable range, respectively, the K_m data have to be interpreted with some caution. However, the plot of log(k_{cat}/K_m) as a function of pH exhibited a bell-shaped profile (not shown), indicating that an ionizable group with a lower pK_a has to be deprotonated and another group with a higher pK_a has to be protonated for optimal catalytic efficiency. Fitting with eq 2 yielded a lower pK_a between 5.8 and 6.5 and a pK_a in the range of 7.3−8.0, depending on the mode of weighting the data errors (statistical or inverse squared).

However, it remains unclear whether the corresponding ionizable groups reside on the free enzyme, the substrate, or both.

Properties of the E76A Variant of Ni-QueD. Glu76 of QueD is part of the strictly conserved cupin motif and thus is assumed to be a ligand to the metal center. In one of the two observed coordination geometries of *A. japonicus* quercetinase, the corresponding E73 residue indeed coordinates the Cu^{2+} cofactor. It also was proposed to act as the general base which removes the proton from the C3 hydroxyl of the flavonol and to modulate the redox potential of the metal ion in the ES complex (*13, 39, 40*). ICP-OES analysis of the QueD E76A protein, purified from cells grown in minimal medium with $NiCl_2$, indicated a metal content of only 0.05 atom of Ni per subunit and small quantities of other metals (Table 1), highlighting the essential role of this residue in metal binding. QueD E76A exhibited marginal quercetinase activity of 0.014 unit/mg, corresponding to a more than 10^4-fold decrease in specific activity. Considering that the QueD E76A protein contains ~10-fold less Ni^{2+} than Ni-QueD, the loss of catalytic activity is remarkably high. It must, however, be interpreted with care, because we cannot exclude the possibility that unspecific adsorption of Ni^{2+} to the enzyme contributes to the measured nickel content.

UV−Vis Spectral Properties of Quercetin and of Anoxic Complexes of Quercetin and Ni- and Co-QueD. Flavonols have two absorption bands, termed band I (with a maximum usually in the range of 350−380 nm) and band II (240−280 nm). Whereas quercetin has a band I absorption maximum at 391 nm (at pH 8 in MES-Tris buffer), absorption of its 2,3-dihydro analogue (taxifolin) in the same buffer is maximal at 325 nm (Figure 4A), indicating that the C2−C3 double bond of quercetin, which confers conjugation of the B-ring and the C4 carbonyl function, is an important determinant of the absorption near the visible range. The UV−vis spectra of quercetin in MES-Tris buffer change as a function of pH. The maximum at 391 nm (pH 8) shifts to 371 and 367 nm at pH 7 and 6, respectively. Band I of quercetin in the presence of a 1.5-fold molar excess of $CoCl_2$ and $NiCl_2$ at pH 8 has a maximum at 404 and 408 nm, respectively, which shifts to 372−373 nm at pH 7 and 367 nm at pH 6. Addition of $CoCl_2$ or $NiCl_2$ to quercetin at pH 8 moreover results in a broadening of band I (Figure 4).

Anoxic addition of a 1.5-fold molar excess of Ni- or Co-QueD holoenzyme to quercetin changed the absorption spectrum of the flavonol, indicating that formation of ES complexes does not require the presence of dioxygen. Remarkably, the quercetin absorption band I shifts to shorter wavelengths in the presence of enzyme, resulting in maxima at 385 nm (with Ni-QueD) and 378 nm (with Co-QueD) at pH 8 (Figure 4). Band I additionally underwent narrowing and, in the case of Co-QueD, splitting in two bands as suggested by the shoulder at 392 nm (Figure 4B). As mentioned above, the UV−vis absorption bands of quercetin undergo hypsochromic shifts when the pH is lowered; however, the spectra at pH 8 of quercetin in the presence of QueD proteins differ from those of quercetin or of Co(II)- and Ni(II)-quercetin complexes at pH 6−8, suggesting that the effect of QueD protein on bound substrate is more complex than a mere shift in the pK_a of quercetin. The hypsochromic shift of band I may indicate that the quercetin chromophore is less conjugated when bound to the enzyme.

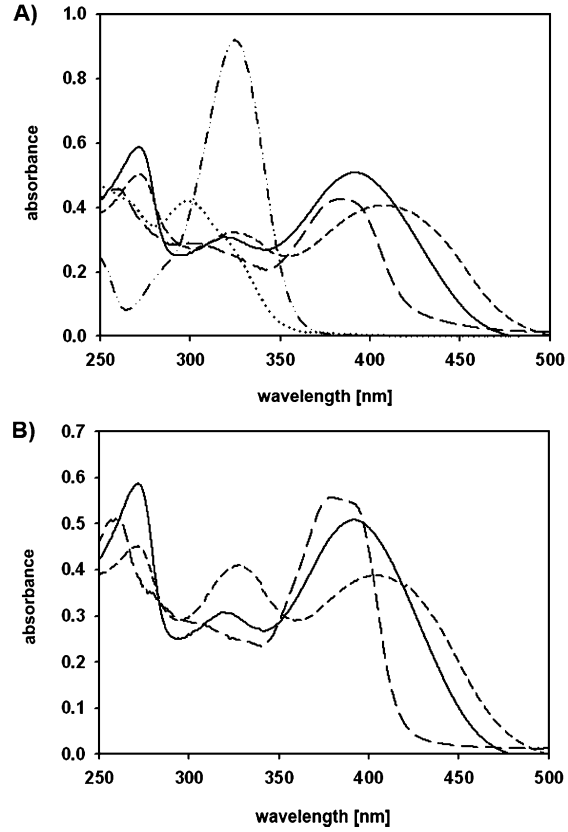

FIGURE 4: UV−vis spectra of quercetin, quercetin and $NiCl_2$ or $CoCl_2$, and quercetin and QueD under anoxic conditions at pH 8. Panels A and B show the spectra of quercetin in buffer (—), quercetin with $NiCl_2$ (A) and $CoCl_2$ (B) (---), and quercetin with Ni-QueD (A) and quercetin with Co-QueD (B) under anoxic conditions (— — —). The dotted−dashed line in panel A represents the UV−vis spectrum of taxifolin, the 2,3-dihydro analogue of quercetin, which illustrates the effect of the C2−C3 double bond on the absorbency of quercetin. The UV−vis spectrum of 2-protocatechuoylphloroglucinol carboxylate, the product of the quercetinase reaction, is represented by the dotted line in panel A. The metal salts and the QueD forms were added at a 1.5-fold molar excess over quercetin (in the case of QueD, the molar excess refers to the amount of holoenzyme as estimated from the metal content of the preparation). All spectra were recorded in 50 mM MES-Tris buffer (pH 8).

Interestingly, the methylation or glucosidation of 3-OH, 5-OH, or 4′-OH, but not 3′-OH or 7-OH, of quercetin also causes a hypsochromic shift of band I (*41*), supporting the notion that the shifts observed for anoxic quercetin−QueD complexes may be due to "tethering" of distinct substituents by the enzyme. Alternatively, or additionally, the "electronic bridge" conferred by the C2−C3 double bond might be affected upon binding of quercetin to the enzyme.

In marked contrast to the spectral changes observed when quercetin interacts with Co- and Ni-QueD, anoxic binding of flavonols to Cu-quercetinase of *Aspergillus flavus* resulted in a bathochromic shift of band I absorption (*11*). In case of ARD, addition of the Ni or Fe form of the enzyme to anoxic solutions of substrate analogues also elicited red shifts of the absorption maxima (*42*). These shifts were proposed to be due to formation of quercetin anion and aci-reductone dianion, respectively, in the ES complexes. However, such anion formation of quercetin in the ES complex cannot be inferred from our UV−vis data.

EPR Spectral Analysis of QueD Proteins. To collect spectroscopic information about the metal sites in Ni-QueD

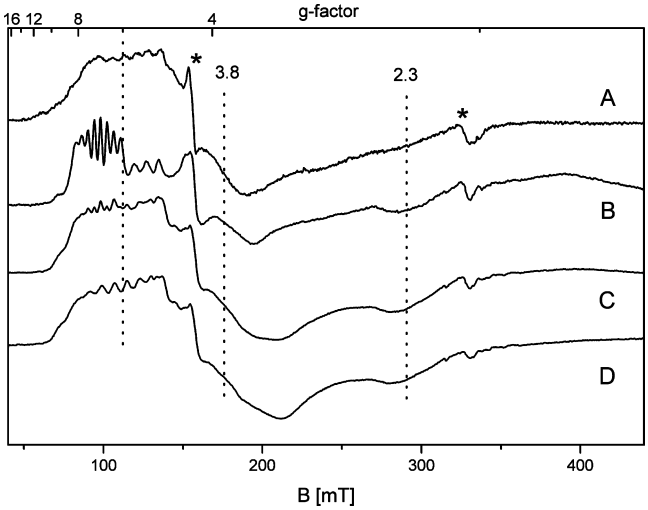

FIGURE 5: EPR spectra of anoxic Co-QueD at 8 K in the resting state (A), after addition of a 3-fold molar excess of quercetin (B), and after being exposed to air for 10 s (C) and 5 min (D). The dotted lines indicate the apparent g factors. The signals marked with asterisks arise from small amounts of adventitious Cu^{2+} ($g \approx 2.05$) and Fe^{3+} ($g \approx 4.3$) in the solution.

and Co-QueD, EPR experiments were performed. Ni-QueD did not exhibit EPR signals indicative of a paramagnetic Ni species under anoxic or oxic conditions and also not in the presence or absence of substrate. Co-QueD samples produced characteristic EPR spectra under all conditions, extending in field from ~50 to ~350 mT (Figure 5). All spectra contained minor $g \approx 2.05$ and $g \approx 4.3$ signals (marked with asterisks in trace A of Figure 5), which presumably arise from traces of Cu^{2+} and Fe^{3+} present in the preparation. The main spectral signatures of Co^{2+} in QueD appear to be grouped in three regions: a broad line at $g \approx 2.3$, a line around $g \approx 3.8$, and a pattern with multiple lines in the region around $g \approx 6$ (indicated by dotted lines in Figure 5). The spectrum of resting Co-QueD recorded at 8 K under anoxic conditions (Figure 5A) is typical for a high-spin ($S = {}^3/_2$) Co^{2+} species also showing barely resolved lines attributable to Co^{2+}−hyperfine (hf) interaction (nuclear spin $I = {}^7/_2$). Comparable spectra have been observed in Co-quercetinase from *B. subtilis* (*21*) and also in Co^{2+}-substituted phospholipase C (*43*). Addition of substrate (in a 3-fold molar excess) leads to drastic changes in the hyperfine pattern at $g \approx 6$, to a shift of the line at $g \approx 3.8$, and to a more pronounced broad line at $g \approx 2.3$ (Figure 5B). A short exposure to air induces a partial decay of the hyperfine pattern as well as a shift and broadening of the line around $g \approx 3.8$; a more prolonged exposure further changes the hyperfine lines (Figure 5C,D).

For a more detailed analysis of the hyperfine patterns, the region around $g \approx 6$ was recorded at a higher field resolution at 8 and 15 K (Figure 6a,b). For resting Co-QueD under anaerobic conditions, six hf lines are clearly visible at both temperatures, and the two low-field hf peaks remain unresolved in the left flank as indicated by the upper stick diagram (S1). The peak distances are between 7.4 and 7.8 mT, and the eight hf lines are then centered at $g = 6.165$ (±0.005) (Figure 6a,b, A traces). At the low-field side of the spectra, there are three additional broad lines of low intensity visible, arising from a second Co−hyperfine interaction. They are separated by ~9.5 mT as indicated by the interpolated corresponding stick diagram (S2, dashed in Figure 6b, trace A) which is centered at about $g = 7.16$ (±0.01). It is noted that identical spectra were obtained for resting Co-QueD in the presence of oxygen (not shown).

In the presence of substrate, the pattern at 15 K (S3) shows some significant changes (Figure 6b, trace B). The hf lines with splitting (S1) identical to that in the resting state are shifted to a higher apparent g value (6.23); the larger coupling of 9.5 mT on the left flank (S2 in trace A) is hardly visible, and on the right flank of the signal, some features are modified as indicated by the arrows. These minor alterations are also found in the spectrum at 8 K, but here, in addition, a new hyperfine pattern of eight lines (S4) is present. Its hf splitting is only 3.9 mT, consisting of lines characteristic of an axial-type component (S4, stick diagram in Figure 6a, trace B) with a corresponding g factor of 6.94. This hf pattern is associated with a fast relaxing Co^{2+} species, because the signal is completely lost above 12 K. A short exposure of the thawed sample to air (for ca. 10 s) induces a decay of the two well-resolved hf patterns (S3 and S4 in trace B), leading to a rather unstructured signal (Figure 6a, trace C). In the spectrum at 15 K, again the lines of axial-type signal S4 with the small hf splitting are missing (Figure 6b, trace C). On the right flank of the signal, an extension to higher fields is noted (marked with asterisks). In the sample further exposed to air (several minutes), signal S4 can no longer be observed (Figure 6a, trace D). Instead, an eight-line hf pattern (S5) is present which differs from signal S1 with respect to the g factor (6.07) and the shape of the hf lines. Here, the splitting is very similar to that in S1, but the central lines exhibit a higher intensity as compared to the outer ones typical for a more axial-type pattern. For both temperatures, also a broad substructure (S6) is apparent in the D spectra which, if associated with a Co^{2+}−hf interaction, has the same splitting as S2 but is shifted to a lower g value (6.43 for S6 vs 7.16).

From this sequence of experiments, several conclusions can be drawn. The overall spectral shape (excluding the hyperfine signals for the moment) in Figure 5 for different states of Co-QueD is not changing drastically. This implies that the spin state ($S = {}^3/_2$) of the metal ion is conserved. The spectral modifications, such as the shift of the signal near $g = 3.8$ or the intensity change of the line at $g = 2.3$, can be associated with alterations of the zero-field splitting parameters (and their variation) in the different states. With respect to spectral intensity, an inspection of the normalized spectra clearly indicates that no drastic loss of signal due to a change in the valency of the Co^{2+} center is occurring. Double integration of the spectra in Figure 5A−D was used to quantitate the relative signal intensities. It was found that the signals nonsystematically vary within ±20% around the average value. This large error is mainly caused by imperfect baseline correction of the highly accumulated spectra. There appears to be no evidence of a change of the valency of the Co ion adopting a diamagnetic state by reduction during substrate turnover.

The analysis of the hyperfine patterns has revealed the presence of several distinct spectral species (S1−S6), which can be associated with different structural and/or functional species, placing the Co ions in slightly modified electronic states. In the resting enzyme, two signal species, S1 and S2, are prevailing with S2 having a lower intensity. At present,

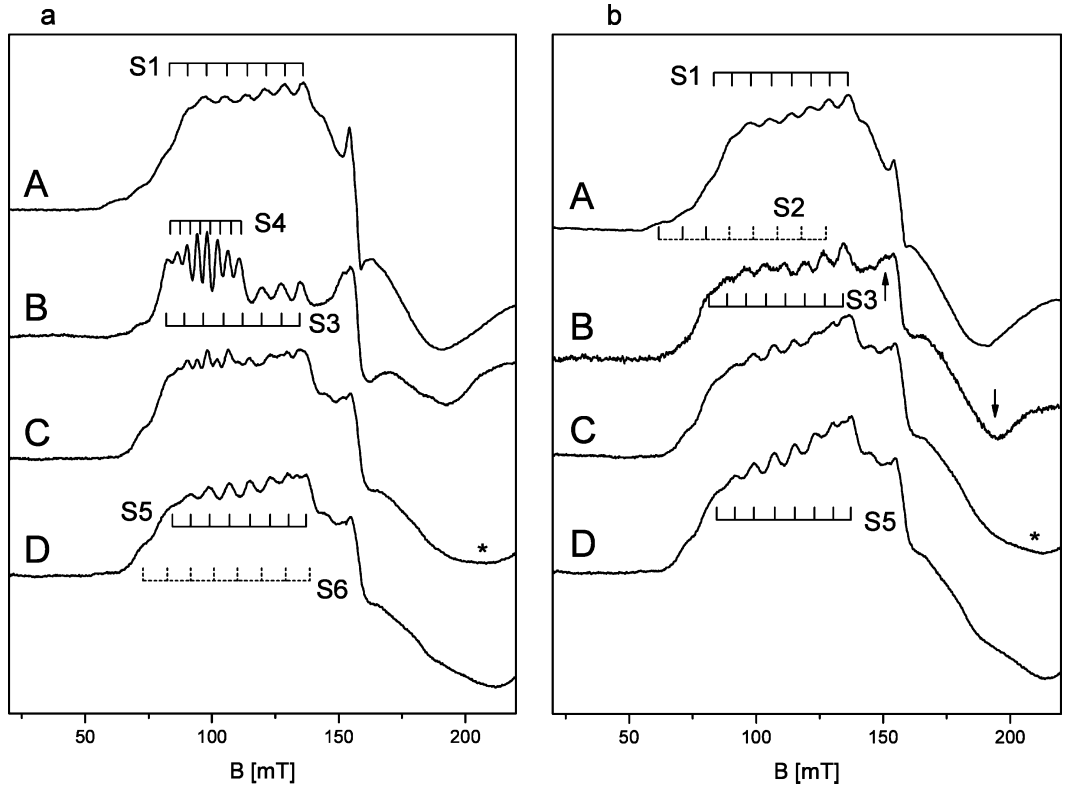

FIGURE 6: EPR spectra of the low-field signal around $g = 6$ of Co-QueD at 8 (a) and 15 K (b) in different states: anoxic resting enzyme (A), after addition of a 3-fold molar excess of quercetin (B), and after being exposed to air for 10 s (C) and 5 min (D). The stick diagrams identify various signals with different apparent g factors and hyperfine couplings. The arrows and asterisks are discussed in the text.

it is not clear if S1 and S2 can be attributed to two Co species sensing a different environment leading to the differences in hyperfine splitting and apparent g factors. Attempts to simulate the spectral pattern were not successful so far but showed that, in principle, contributions of different **g**- and **A**-tensor components associated with different zero-field splitting may produce overlapping hyperfine lines. However, it is evident that signals S3 and S4, appearing upon addition of the substrate, can be associated with a substrate bound within or close to the ligand sphere of the Co ion, obviously affecting the g and hyperfine values as well as the zero-field parameters and relaxation properties. The surprisingly small hyperfine coupling of signal S4 (3.9 mT) may be indicative of delocalization of spin population away from the Co ion onto the substrate, which might then reflect a polarization of the substrate bound to the Co ion. After the reaction was started by allowing access of oxygen, the signal of the substrate-bound species decays, and a new signal S5 (and possibly S6) appears, which therefore can be related to a product-bound state of the Co ion or to a state after release of product, but not identical to the resting state. Trials to remove product by repeated washing with buffer and to recover the resting state (S1) unfortunately left the enzyme in an undefined state. Cobalt signals very similar to S1 were present, but a considerable portion of the metal ions produced an unusual axial signal at $g = 3.4$.

The interpretation of the high-spin Co^{2+} EPR spectra regarding the symmetry of the ion (i.e., its coordination sphere) is rather elusive due to the complexity introduced by the zero-field parameters, but some comparison can be made with model complexes of defined structure. From these studies, we concluded mainly on the basis of hyperfine couplings that values below ~10 mT are indicative for tetrahedral or trigonal bipyramidal complexes (*44, 45*). Because the hyperfine values for Co-QueD are in a range between 9.5 and 3.9 mT, it appears that a tetrahedral or trigonal bipyramidal geometry of the Co ion is prevailing. For comparison, the Cu^{2+} ion in *A. japonicus* quercetinase exhibits two distinct geometries, a main, distorted tetrahedral coordination by three histidine residues and a water ligand and a minor, distorted trigonal bipyramidal conformation with an additional glutamate ligand (*13, 39*). The Fe^{2+} in the N-terminal active site of *Bacillus* quercetinase was assigned to have a distorted trigonal bipyramidal coordination geometry, whereas tetrahedral coordination was observed in the C-terminal domain (*18*). The Mn^{2+} form of *Bacillus* quercetinase exhibits an octahedral coordination (*21*). In both Fe- and Ni-ARD, the metal ion is bound in a pseudo-octahedral geometry with the same set of N/O ligands (*24, 46*).

DISCUSSION

Protein subunits of the functionally very diverse cupin superfamily can consist of a single cupin domain or have a bicupin or multicupin domain structure (*19*). Dioxygenases are found in both the monocupin and bicupin subset. In the bicupin scaffold of *A. japonicus* quercetinase, the linker connecting the C- and N-terminal domains features a flexible region, which gains order upon substrate binding (*40*). In case of *Bacillus* quercetinase, the two cupin domains of each subunit are joined by a flexible loop, which forms the lid of the active site of the N-terminal domain (*18*). As an enzyme composed of monocupin subunits, *Streptomyces* QueD may lack an analogous structural element.

Among the plethora of oxygenases within the cupin superfamily, most enzymes contain iron as the active site

metal (*19*). The quercetinases described so far contain copper (*Aspergillus*) or are somewhat promiscuous with respect to their metal cofactor (*Bacillus*). *Streptomyces* QueD is most active with nickel ions and thus represents the second example of a nickel-containing cupin besides Ni-ARD. It is noteworthy that from a physiological point of view as well as with respect to the protein fold (*23*), the iron form of ARD, which is part of the methionine salvage pathway, seems to represent the "default" enzyme whereas the biological significance of Ni-ARD remains unclear.

The metal occupancy of Co- and Ni-QueD purified from recombinant *E. coli* was in the range of 50%. Similarly, the Co form of *Bacillus* quercetinase, purified from recombinant *E. coli*, contained 0.65 metal atom per bicupin subunit, although it can bind two metal ions per subunit (*21*). In both cases, metal deficiency of the recombinant proteins could be due to extensive protein overproduction by the expression systems (*15*). Metal uptake by the cells and its incorporation into the nascent QueD apoprotein are probably the limiting factors for assembly of the native holoenzyme. Moreover, metal homeostasis probably is tightly controlled in *E. coli*. Outten and O'Halloran reported that intracellular Co and Ni could not be detected in *E. coli* under normal growth conditions, in contrast to Cu, Mn, Fe, and Zn, the latter two being the most abundant metals in the *E. coli* cell (*34*).

The apparent K_m values of recombinant *Streptomyces* QueD for quercetin and for dioxygen depend on the nature of the metal cofactor, suggesting that the metal ion or subtle conformational changes induced by the metal ion affect substrate binding. In contrast, the K_m values of the Mn, Co, and Fe forms of *Bacillus* quercetinase for quercetin were similar and in the range of 4.0−7.5 μM (*21*). The $k_{cat,app}$ values for quercetin of the Co forms of the *Bacillus* and *Streptomyces* enzymes are almost identical ($\sim$8 s^{-1}), and those of the respective Fe forms of the two proteins are also similar. However, the two enzymes perform differently with Ni^{2+}, which is a poor cofactor of the *Bacillus* enzyme (*21*). Considering the higher k_{cat} values of the Ni form for quercetin and its lower K_m for dioxygen, Ni-QueD should be superior to Co-QueD under physiological conditions, provided that the concentration of the organic substrate is in the micromolar range. It is interesting to note that in a tetrahedral ligand field, the Lewis acidity of Co(II) is expected to be higher than that of Ni(II) (*47*). An increased affinity of the Co(II) center of Co-QueD for organic ligands might rationalize its comparatively low K_m for quercetin.

Oxygenases have to activate dioxygen, and/or their organic substrate, for the reaction to occur. Molecular oxygen as a consequence of its electronic structure is kinetically inert and has a significant activation barrier to reaction. Its electronic ground state has two unpaired electrons in the highest occupied molecular orbitals (HOMO), contributing to an $S = 1$ total spin. This results in an unfavorable potential for the one-electron reduction of O_2 to the superoxide anion radical [−330 mV at pH 7 and unit pressure (*48*)], imparting a "thermodynamic barrier". Moreover, the direct reaction of triplet oxygen with a singlet organic molecule (spin-paired, $S = 0$) to form singlet-state products would violate a fundamental principle of physics, the conservation of angular momentum, and thus imparts a "spin barrier". For an organic molecule to react with dioxygen, a catalyst has to overcome or circumvent these barriers. In enzymes, this can be achieved by orbital overlap with a suitable transition metal ion or by electron transfer from a potent electron donor to form an enzyme-bound reduced oxygen species.

The preference of QueD for Ni^{2+} or Co^{2+} is very unusual, if not unique, for oxygenases, raising the question of whether the metal ions in the expected ligand environment of QueD have a redox role in dioxygen activation. For Ni-ARD, the only other Ni-containing dioxygenase, a nonredox role for the Ni(II) center has been discussed, because XAS studies did not reveal evidence of a change in redox state upon substrate binding and because the nickel ion in a N/O donor ligand environment is not expected to have biochemically accessible redox chemistry (*49, 50*). In this study, we performed EPR studies on Co-QueD to probe its redox behavior. The EPR spectrum of the resting enzyme was not affected by the presence of dioxygen, clearly arguing against a direct reaction of the Co(II) center with O_2 to form a Co(III)−superoxide complex. Interestingly, anoxic binding of quercetin to Co-QueD has geometric effects on the metal site and causes significant redistribution of electron density in the ES complex (as also indicated by UV−vis spectroscopy), but the cobalt ion maintains a formal Co(II) oxidation state. This finding suggests that electron transfer reactions between Co(II) and bound quercetin do not occur. In this context, it is interesting to note that in trigonal bipyramidal high-spin Co(II) complexes with a 3N,1O ligand environment, the Co(II) state is stabilized (*51*), supporting the notion that the redox potential of the Co(III)/Co(II) pair is outside the range required for donation of an electron to dioxygen, or to the flavonol. For the reduction potentials of the flavonoid radical of quercetin, values (vs SHE) of −37, 90, and 330 mV were observed in aqueous solution at pH 13.5, 10.8, and 7.0, respectively (*52*). Even if reduction potentials of metal centers as well as of bound substrates are usually significantly influenced by the protein environment, a role of the Co(II) center of QueD as the electron donor appears unlikely. Dismissal of a possible role of Co(II) as an electron donor raises the question of whether Co(II) contrariwise could undergo reduction during catalysis. Even if the EPR data clearly show that formation of a Co(I) state upon binding of quercetin to Co-QueD does not occur, we cannot fully exclude the possibility that electron transfer from the organic substrate via the metal to dioxygen is triggered by dioxygen binding. If such a transient change of the oxidation state of the metal center were followed by a fast step in the catalytic reaction, it would not be detected by conventional EPR but would require pre-steady-state kinetic methods for analysis.

The organic chemistry of the reaction of flavonols with dioxygen has been studied intensely, and the reaction catalyzed by quercetinase actually can be mimicked by different model reactions. In aprotic solvents, flavonolate complexes with Cu(I) and Cu(II) (*53*) as well as cobalt complexes (*54, 55*) proved to catalyze the oxygenation of flavonolate to CO and the depside. Interestingly, however, basic conditions and the presence of dioxygen are sufficient for selective 2,4-dioxygenolysis of flavonols, demonstrating that a metal catalyst is not necessarily required for the reaction of flavonolate with dioxygen (*37, 53, 56*). Oxygenolysis is fast in aprotic solvents and slows in aqueous solution (*37*). EPR analysis of the base-catalyzed dioxygenolysis of flavonol in DMF showed the presence of a flavonoxyl radical, which results from single-electron transfer from the flavono-

late to dioxygen (*53*), indicating that the flavonolate anion itself has the reducing power to donate an electron to dioxygen.

Alternatively with respect to a radical mechanism via a flavonoxy−superoxide radical pair, the hypothesis of an ionic mechanism has been discussed for the chemical dioxygenolysis of flavonols, suggesting that due to the high energy level of the HOMO orbital of the flavonolate, a direct electrophilic attack of $^3O_2$ on the flavonolate anion is possible (*53, 55*). Whereas in the radical mechanism, the spin restriction of the reaction of singlet substrate with $^3O_2$ is overcome by spin inversion in the superoxide radical, which allows radical recombination, the second route depends on the high energy content of the flavonolate and involves intersystem crossing between a triplet charge-transfer complex and a singlet charge-transfer complex (*55*).

Remarkably, the dianion (pH 13) of an aci-reductone model substrate of ARD also undergoes nonenzymatic oxidation in the presence of O_2 (*42*). In view of the chemical reactivity of the aci-reductone dianion and of flavonolate anions toward dioxygen, a crucial role of the enzyme catalyst might be to abstract a proton from the substrate to form a reactive enzyme-bound anion. In *Aspergillus* quercetinase, glutamate residue E73, which also is a ligand to the copper ion, was proposed to initiate catalysis by abstraction of a proton from the 3-OH group of the flavonol (*13, 39*). A corresponding glutamate residue (E76) is conserved in *Streptomyces* quercetinase; however, the properties of the E76A variant of QueD could not shed light on the potential catalytic role of this residue. Interestingly, the possibility of a histidine residue or a hydroxy ligand as a catalytic base have been discussed for Ni-ARD (*49*). The pH dependence of $k_{cat,app}$ of QueD tentatively suggested that in the ES complex an ionizable group with a pK_a of ~6.8 has to be deprotonated for catalysis to occur, but clear assignment to a catalytic base is not possible based on these data.

Taken together, the biochemical and spectroscopic data on QueD, considerations on single-electron redox potentials of cobalt complexes, O_2, and quercetin, and the chemical mechanism of model reactions suggest the possibility of a nonredox role of the metal cofactor of QueD. Construction and structural and functional characterization of QueD forms harboring a redox-inert metal ion such as Zn^{2+} could shed light on this hypothesis. Interestingly, ring cleavage dioxygenases active toward 3-hydroxy-4(1*H*)-quinolones, which like quercetinases catalyze a 2,4-dioxygenolytic ring cleavage of their heterocyclic substrate with formation of carbon monoxide, neither require nor contain a metal ion or an organic cofactor for catalysis (*57, 58*). In general, different cofactor-independent oxygenases seem to have in common the fact that base-catalyzed abstraction of a proton from the substrate is an initial step of the catalytic reaction (*58*−*60*). Their substrates (in their anionic forms) are presumed to have a high reducing power and are thought to directly transfer an electron to dioxygen to form a substrate radical−superoxide pair, but it should be emphasized that direct experimental evidence of the presence of an enzyme-bound radical pair in cofactor-independent oxygenases is lacking. However, a common feature of the organic substrates of cofactor-less oxygenases, shown in chemical model reactions, is their ability to form resonance-stabilized radicals, which is a prerequisite for the proposed mechanistic pathway. On the basis of the chemical properties of quercetin discussed above, and the presumed redox inertness of the metal center of Co-QueD, an analogous reaction pathway, i.e., direct electron transfer from the activated flavonol to dioxygen without the need for redox cycling of the metal, may be envisaged for the reaction catalyzed by Ni- and Co-QueD. The major role of the divalent metal ion in the active site of QueD could be to control the orientation of bound substrates, to contribute to modulating the reduction potential of the bound flavonol, and to provide electrostatic stabilization of anionic intermediates, rather than to participate directly in redox chemistry.

ACKNOWLEDGMENT

We thank Dr. Heinrich Luftmann, Institute of Organic Chemistry, University of Münster, for mass spectrometrical analyses. On the occasion of his recent retirement, we (S.F. and R.K.) express our gratitude to Prof. Dr. J. Hüttermann for his continuous support in a longstanding and fruitful cooperation.

REFERENCES

1. Iwashina, T. (2000) The structure and distribution of the flavonoids in plants. *J. Plant Res. 113*, 287–299.
2. Pietta, P.-G. (2000) Flavonoids as antioxidants. *J. Nat. Prod. 63*, 1035–1042.
3. Cushnie, T. P. T., and Lamb, A. J. (2005) Antimicrobial activity of flavonoids. *Int. J. Antimicrob. Agents 26*, 343–356.
4. Hartwig, U. A., Joseph, C. M., and Phillips, D. A. (1991) Flavonoids released naturally from alfalfa seeds enhance growth rate of *Rhizobium meliloti*. *Plant Physiol. 95*, 797–803.
5. Stevens, J. F., Wollenweber, E., Ivancic, M., Hsu, V. L., Sundberg, S., and Deinzer, M. L. (1999) Leaf surface flavonoids of *Chrysothamnus*. *Phytochemistry 51*, 771–780.
6. Kalinova, J., Vrchotova, N., and Triska, J. (2007) Exudation of allelopathic substances in buckwheat (*Fagopyrum esculentum* Moench). *J. Agric. Food Chem. 55*, 6453–6459.
7. Westlake, D. W. S., Roxburgh, J. M., and Talbot, G. (1961) Microbial production of carbon monoxide from flavonoids. *Nature 189*, 510–511.
8. Schultz, E., Engle, F. E., and Wood, J. M. (1974) New oxygenases in degradation of flavones and flavanones by *Pseudomonas putida*. *Biochemistry 13*, 1768–1776.
9. Rao, J. R., and Cooper, J. E. (1994) Rhizobia catabolize *nod* gene-inducing flavonoids via C-ring fission mechanisms. *J. Bacteriol. 176*, 5409–5413.
10. Schneider, H., and Blaut, M. (2000) Anaerobic degradation of flavonoids by *Eubacterium ramulus*. *Arch. Microbiol. 173*, 71–75.
11. Oka, T., Simpson, F. J., and Krishnamurty, H. G. (1972) Degradation of rutin by *Aspergillus flavus*: Studies on specificity, inhibition, and possible reaction mechanism of quercetinase. *Can. J. Microbiol. 18*, 493–508.
12. Hund, H. K., Breuer, J., Lingens, F., Hüttermann, J., Kappl, R., and Fetzner, S. (1999) Flavonol 2,4-dioxygenase from *Aspergillus niger* DSM 821, a type 2 Cu-II-containing glycoprotein. *Eur. J. Biochem. 263*, 871–878.
13. Fusetti, F., Schröter, K. H., Steiner, R. A., van Noort, P. I., Pijning, T., Rozeboom, H. J., Kalk, K. H., Egmond, M. R., and Dijkstra, B. W. (2002) Crystal structure of the copper-containing quercetin 2,3-dioxygenase from *Aspergillus japonicus*. *Structure 10*, 259–268.
14. Bowater, L., Fairhurst, S. A., Just, V. J., and Bornemann, S. (2004) *Bacillus subtilis* YxaG is a novel Fe-containing quercetin 2,3-dioxygenase. *FEBS Lett. 557*, 45–48.
15. Barney, B. M., Schaab, M. R., LoBrutto, R., and Francisco, W. A. (2004) Evidence for a new metal in a known active site: Purification and characterization of an iron-containing quercetin 2,3-dioxygenase from *Bacillus subtilis*. *Protein Expression Purif. 35*, 131–141.
16. Merkens, H., Sielker, S., Rose, K., and Fetzner, S. (2007) A new monocupin quercetinase of *Streptomyces* sp. FLA: Identification and heterologous expression of the *queD* gene and activity of the

recombinant enzyme towards different flavonols. *Arch. Microbiol. 187*, 475–487.
17. Tranchimand, S., Ertel, G., Gaydou, V., Gaudin, C., Tron, T., and Iacazio, G. (2008) Biochemical and molecular characterization of a quercetinase from *Penicillium olsonii*. *Biochimie 90*, 781–789.
18. Gopal, B., Madan, L. L., Betz, S. F., and Kossiakoff, A. A. (2005) The crystal structure of a quercetin 2,3-dioxygenase from *Bacillus subtilis* suggests modulation of enzyme activity by a change in the metal ion at the active site(s). *Biochemistry 44*, 193–201.
19. Dunwell, J. M., Purvis, A., and Khuri, S. (2004) Cupins: The most functionally diverse protein superfamily? *Phytochemistry 65*, 7–17.
20. Kooter, I. M., Steiner, R. A., Dijkstra, B. W., van Noort, P. I., Egmond, M. R., and Huber, M. (2002) EPR characterization of the mononuclear Cu-containing *Aspergillus japonicus* quercetin 2,3-dioxygenase reveals dramatic changes upon anaerobic binding of substrates. *Eur. J. Biochem. 269*, 2971–2979.
21. Schaab, M. R., Barney, B. M., and Francisco, W. A. (2006) Kinetic and spectroscopic studies on the quercetin 2,3-dioxygenase from *Bacillus subtilis*. *Biochemistry 45*, 1009–1016.
22. Dai, Y., Wensink, P. C., and Abeles, R. H. (1999) One protein, two enzymes. *J. Biol. Chem. 274*, 1193–1195.
23. Ju, T. T., Goldsmith, R. B., Chai, S. C., Maroney, M. J., Pochapsky, S. S., and Pochapsky, T. C. (2006) One protein, two enzymes revisited: A structural entropy switch interconverts the two isoforms of acireductone dioxygenase. *J. Mol. Biol. 363*, 823–834.
24. Pochapsky, T. C., Pochapsky, S. S., Ju, T. T., Mo, H. P., Al-Mjeni, F., and Maroney, M. J. (2002) Modeling and experiment yields the structure of acireductone dioxygenase from *Klebsiella pneumoniae*. *Nat. Struct. Biol. 9*, 966–972.
25. Sambrook, J., Fritsch, E. F., and Maniatis, T. (1989) *Molecular Cloning: A Laboratory Manual*, 2nd ed., Cold Spring Harbor Laboratory Press, Plainview, NY.
26. Schlegel, H. G., Kaltwasser, H., and Gottschalk, G. (1961) Ein Submersverfahren zur Kultur wasserstoffoxydierender Bakterien: Wachstumsphysiologische Untersuchungen. *Arch. Mikrobiol. 38*, 209–222.
27. Pfennig, N. (1974) *Rhodopseudomonas globiformis*, sp. n., a new species of the Rhodospirillaceae. *Arch. Microbiol. 100*, 197–206.
28. Zor, T., and Selinger, Z. (1996) Linearization of the Bradford protein assay increases its sensitivity: Theoretical and experimental studies. *Anal. Biochem. 236*, 302–308.
29. Pace, C. N., Vajdos, F., Fee, L., Grimsley, G., and Gray, T. (1995) How to measure and predict the molar absorption coefficient of a protein. *Protein Sci. 4*, 2411–2423.
30. Laemmli, U. K. (1970) Cleavage of structural proteins during the assembly of the head of bacteriophage T4. *Nature 227*, 680–685.
31. Cornish-Bowden, A. (2004) *Fundamentals of Enzyme Kinetics*, 3rd ed., Portland Press Ltd., London.
32. Friedemann, T. E., and Haugen, G. E. (1943) Pyruvic acid. II. The determination of keto acids in blood and urine. *J. Biol. Chem. 147*, 415–442.
33. Andrade, M. A., Chacón, P., Merelo, J. J., and Morán, F. (1993) Evaluation of secondary structure of proteins from UV circular dichroism spectra using an unsupervised learning neural network. *Protein Eng. 6*, 383–390.
34. Outten, C. E., and O'Halloran, T. V. (2001) Femtomolar sensitivity of metalloregulatory proteins controlling zinc homeostasis. *Science 292*, 2488–2492.
35. Perczel, A., Park, K., and Fasman, G. D. (1992) Deconvolution of the circular dichroism spectra of proteins: The circular dichroism spectra of the antiparallel β-sheet in proteins. *Proteins 13*, 57–69.
36. Jungbluth, G., Rühling, I., and Ternes, W. (2000) Oxidation of flavonols with Cu(II), Fe(II) and Fe(III) in aqueous media. *J. Chem. Soc., Perkin Trans. 2,* 1946–1952.
37. Nishinaga, A., Tojo, T., Tomita, H., and Matsuura, T. (1979) Base-catalyzed oxygenolysis of 3-hydroxyflavones. *J. Chem. Soc., Perkin Trans. 1,* 2511–2516.
38. Escandar, G. M., and Sala, L. F. (1991) Complexing behavior of rutin and quercetin. *Can. J. Chem. 69*, 1994–2001.
39. Steiner, R. A., Kooter, I. M., and Dijkstra, B. W. (2002) Functional analysis of the copper-dependent quercetin 2,3-dioxygenase. 1. Ligand-induced coordination changes probed by X-ray crystallography: Inhibition, ordering effect, and mechanistic insights. *Biochemistry 41*, 7955–7962.
40. Steiner, R. A., Kalk, K. H., and Dijkstra, B. W. (2002) Anaerobic enzyme-substrate structures provide insight into the reaction mechanism of the copper-dependent quercetin 2,3-dioxygenase. *Proc. Natl. Acad. Sci. U.S.A. 99*, 16625–16630.
41. Day, A. J., Bao, Y., Morgan, M. R. A., and Williamson, G. (2000) Conjugation position of quercetin glucuronides and effect on biological activity. *Free Radical Biol. Med. 29*, 1234–1243.
42. Dai, Y., Pochapsky, T. C., and Abeles, R. H. (2001) Mechanistic studies of two dioxygenases in the methionine salvage pathway of *Klebsiella pneumoniae*. *Biochemistry 40*, 6379–6387.
43. Bicknell, R., Hanson, G. R., Holmquist, B., and Little, C. (1986) A spectral study of cobalt(II)-substituted *Bacillus cereus* phospholipase C. *Biochemistry 25*, 4219–4223.
44. Bencini, A., Bertini, I., Canti, G., Gatteschi, D., and Luchinat, C. (1981) The EPR spectra of the inhibitor derivatives of cobalt carbonic anhydrase. *J. Inorg. Biochem. 14*, 81–93.
45. Makinen, M. W., Kuo, L. C., Yim, M. B., Wells, G. B., Fukuyama, J. M., and Kim, J. E. (1985) Ground term splitting of high-spin Co^{2+} as a probe of coordination structure. 1. Dependence of the splitting on coordination geometry. *J. Am. Chem. Soc. 107*, 5245–5255.
46. Chai, S. C., Ju, T. T., Dang, M., Goldsmith, R. B., Maroney, M. J., and Pochapsky, T. C. (2008) Characterization of metal binding in the active sites of acireductone dioxygenase isoforms from *Klebsiella* ATCC 8724. *Biochemistry 47*, 2428–2438.
47. Dunn, M. F., Dietrich, H., MacGibbon, A. K. H., Koerber, S. C., and Zeppezauer, M. (1982) Investigation of intermediates and transition states in the catalytic mechanisms of active site substituted cobalt(II), nickel(II), zinc(II), and cadmium(II) horse liver alcohol dehydrogenase. *Biochemistry 21*, 354–363.
48. Sawyer, D. T., and Valentine, J. S. (1981) How super is superoxide? *Acc. Chem. Res. 14*, 393–400.
49. Al-Mjeni, F., Ju, T., Pochapsky, T. C., and Maroney, M. J. (2002) XAS investigation of the structure and function of Ni in acireductone dioxygenase. *Biochemistry 41*, 6761–6769.
50. Maroney, M. J. (1999) Structure/function relationships in nickel metallobiochemistry. *Curr. Opin. Chem. Biol. 3*, 188–199.
51. Scarpellini, M., Wu, A. J., Kampf, J. W., and Pecoraro, V. L. (2005) Corroborative models of the cobalt(II) inhibited Fe/Mn superoxide dismutases. *Inorg. Chem. 44*, 5001–5010.
52. Jovanovic, S. V., Steenken, S., Hara, Y., and Simic, M. G. (1996) Reduction potentials of flavonoid and model phenoxyl radicals. Which ring in flavonoids is responsible for antioxidant activity. *J. Chem. Soc., Perkin Trans. 2,* 2497–2504.
53. Kaizer, J., Balogh-Hergovich, E., Czaun, M., Csay, T., and Speier, G. (2006) Redox and nonredox metal assisted model systems with relevance to flavonol and 3-hydroxyquinolin-4(1*H*)-one 2,4-dioxygenase. *Coord. Chem. Rev. 250*, 2222–2233.
54. Nishinaga, A., Tojo, T., and Matsuura, T. (1974) A model catalytic oxygenation for the reaction of quercetinase. *J. Chem. Soc., Chem. Commun.,* 896–897.
55. Nishinaga, A., Kuwashige, T., Tsutsui, T., Mashino, T., and Maruyama, K. (1994) On the mechanism of a model quercetinase reaction using a cobalt Schiff-base complex. *J. Chem. Soc., Dalton Trans.,* 805–810.
56. Nishinaga, A., and Matsuura, T. (1973) Base-catalyzed autoxidation of 3,4′-dihydroxyflavone. *J. Chem. Soc., Chem. Commun.,* 9–10.
57. Fetzner, S. (2002) Oxygenases without requirement for cofactors or metal ions. *Appl. Microbiol. Biotechnol. 60*, 243–257.
58. Frerichs-Deeken, U., Ranguelova, K., Kappl, R., Hüttermann, J., and Fetzner, S. (2004) Dioxygenases without requirement for cofactors, and their chemical model reaction: Compulsory order ternary complex mechanism of 1*H*-3-hydroxy-4-oxoquinaldine 2,4-dioxygenase involving general base catalysis by histidine 251 and single-electron oxidation of the substrate dianion. *Biochemistry 43*, 14485–14499.
59. Widboom, P. F., Fielding, E. N., Liu, Y., and Bruner, S. D. (2007) Structural basis for cofactor-independent dioxygenation in vancomycin biosynthesis. *Nature 447*, 342–345.
60. Fetzner, S. (2007) Cofactor-independent oxygenases go it alone. *Nat. Chem. Biol. 3*, 374–375.

BI801398X